



Delft University of Technology

## Oscillation of a graphene flake on an undulated substrate with amplitude gradient

Bian, Jianjun; Nicola, Lucia

**DOI**

[10.1016/j.commatsci.2022.111522](https://doi.org/10.1016/j.commatsci.2022.111522)

**Publication date**

2022

**Document Version**

Final published version

**Published in**

Computational Materials Science

**Citation (APA)**

Bian, J., & Nicola, L. (2022). Oscillation of a graphene flake on an undulated substrate with amplitude gradient. *Computational Materials Science*, 211, Article 111522. <https://doi.org/10.1016/j.commatsci.2022.111522>

**Important note**

To cite this publication, please use the final published version (if applicable). Please check the document version above.

**Copyright**

Other than for strictly personal use, it is not permitted to download, forward or distribute the text or part of it, without the consent of the author(s) and/or copyright holder(s), unless the work is under an open content license such as Creative Commons.

**Takedown policy**

Please contact us and provide details if you believe this document breaches copyrights. We will remove access to the work immediately and investigate your claim.



## Full Length Article

## Oscillation of a graphene flake on an undulated substrate with amplitude gradient

Jianjun Bian<sup>a,b</sup>, Lucia Nicola<sup>a,c,\*</sup><sup>a</sup> Department of Industrial Engineering, University of Padova, Via Gradenigo 6/a, 35131, Padua, Italy<sup>b</sup> Department of Engineering Mechanics, SVL, Xi'an Jiaotong University, Xi'an 710049, PR China<sup>c</sup> Department of Material Science and Engineering, Delft University of Technology, Delft, The Netherlands

## ARTICLE INFO

## Keywords:

Graphene flake

Undulation gradient

Oscillator

## ABSTRACT

The oscillation of a graphene flake on a substrate with undulated surface is investigated by classical molecular dynamics simulation. The gradient in amplitude of the undulation is found to provide the driving force for the motion of the graphene flake, which slides on top of a graphene layer that well conforms to the substrate. The oscillatory motion of the flake can be well described by the equation of motion of a damped oscillator, with damping factor corresponding to the friction coefficient between the flake and the graphene layer on which it glides. When the amplitude gradient increases, the oscillation frequency increases as well. The shape of the graphene flake is found to have a strong influence on friction, as some geometries promote in-plane rotation. The results in the present study point to an alternative approach to transport or manipulation of nanosized objects.

## 1. Introduction

Manipulating or transporting nanosized objects is an intriguing research topic, which has a great application potential in the fields of nanorobotics, nanoscale cargoes and motors [1–7]. A way to drive the movement of nanosized objects is to introduce an external or internal potential field around the object. Commonly used approaches involve the application of an external electrical, optical or acoustic field to initiate the motion [8,9]. For instance, with the aid of an electrical field, water can be pumped through carbon nanotubes [8], and the diffusion of the chiral nanoparticles can be manipulated by external acoustic or optical fields [9]. However, these approaches require complex multiphysical setups. Alternative methods include the introduction of a chemical potential gradient on a chemically modified surface or a temperature gradient to induce the movements of nanodroplets and carbon-based nanostructures [5,10–12]. Also, purely mechanical approaches have been recently developed, where the gradients of mechanical properties or deformation are introduced to supply a driving force. For instance, a tapered nanoscale channel can be used to guide the motion of nanotubes [13]. Similarly, graphene substrates with a stretch-induced strain gradient or with a displacement-induced curvature gradient could be used to precisely transport molecular mass [14,15]. It was discovered that nanoscale sliders on a graphene substrate move toward the region of higher stiffness, therefore its motion can

be manipulated through changing the stiffness gradient of the substrate [16]. Additionally, the potential gradient deriving from some specially designed nanostructures, as the Archimedean-like spiral-shaped carbon nanotubes [17], provides the driving force that supports its use as a nano-oscillator.

Surfaces can now be patterned with tiny features that can be precisely constructed and tuned at the micro and even nano-meter scale [18–21]. For example, surfaces can be patterned as a collection of micropillars, and used to initiate the motion of fluid droplets when the micropillars of similar height but various cross-sectional area [20]. Motivated by these studies, we demonstrate that the amplitude gradient of an undulated rough surface can provide the driving force for the motion of a nanosized flake. In this study, an undulated copper surface covered by a graphene layer serves as the substrate, and the movement of a graphene flake on it is investigated by classical molecular dynamics (MD) simulations.

## 2. Methodology and materials

The constituents of the atomistic model, presented in Fig. 1, are a copper substrate with an undulated surface of varying amplitude, a single pristine graphene layer, and a square-shape graphene flake. The dimensions of the copper substrate are  $10.0 \times 60.0 \times 1.0 \text{ nm}^3$ .

\* Corresponding author at: Department of Industrial Engineering, University of Padova, Via Gradenigo 6/a, 35131, Padua, Italy.  
E-mail address: [lucia.nicola@unipd.it](mailto:lucia.nicola@unipd.it) (L. Nicola).

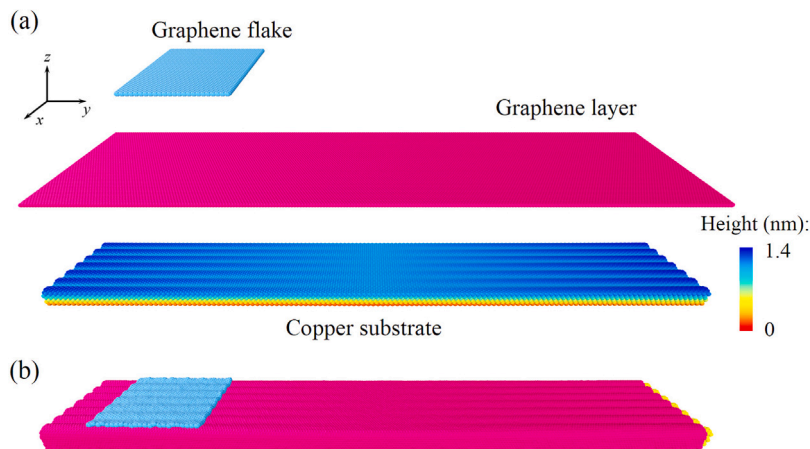


Fig. 1. (a) The constituents of the model: the undulated copper substrate with an amplitude gradient, graphene layer and graphene flake. (b) The full model after positioning the graphene layer on top of the copper substrate, and the graphene flake on the graphene layer.

To prepare the undulated substrate, a thin layer of copper single crystal of lattice constant  $a = 3.615 \text{ \AA}$  is first constructed. The origin of the Cartesian coordinate system is set to be in the middle of the substrate. The lattice is oriented such that the  $[1\bar{1}0]$ ,  $[11\bar{2}]$  and  $[111]$  directions correspond to the  $x$ -,  $y$ - and  $z$ -directions, respectively. The surface topography is obtained by displacing the atoms of the substrate such that the surface profile fulfills the following equation:

$$z(x, y) = A(y)\cos(\omega x) + A(y), \quad (1)$$

where  $\omega$  represents the frequency of the sinusoidal wave along the  $x$ -direction [22,23]. To realize the amplitude gradient along the  $y$ -direction,  $A(y)$  is chosen as a function which linearly decays from the two ends of the substrate to the middle, and has the form

$$A(y) = \begin{cases} -gy, & y \leq 0 \\ gy, & y > 0 \end{cases} \quad (2)$$

where,  $g$  is the amplitude gradient, that we herein assume to be constant. To simplify the simulation and model, the copper substrate is then taken to behave as a rigid body. The graphene layer is 24.0 nm wide in the  $x$ -direction and the same size as the copper substrate along the  $y$ -direction. The zigzag direction of the graphene layer is along the  $x$ -direction, and the arm-chair direction is along the  $y$ -direction. The edge length of the square-shape flake is 9.8 nm, a bit smaller than the width of the substrate. To prevent the formation of a commensurate state between the flake and the graphene layer, the zigzag direction of the flake is taken along the  $y$ -axis, the arm-chair direction along the  $x$ -axis. Fig. 1a depicts the atomic configurations of the substrate, the graphene layer, and the flake before relaxation.

The covalent carbon-carbon bonds in the graphene layer and the flake are described by the Adaptive Interatomic Reactive Empirical Bond Order (AIREBO) potential [24]. The Van der Waals interactions between the graphene layer and the copper substrate, and those between the flake and the graphene layer are described by the classical 6–12 pairwise Lennard-Jones (LJ) potential. The LJ parameters for the copper substrate-graphene interaction are adopted from previous work [25] with a well-depth of  $\epsilon = 27.58 \text{ meV}$  and an equilibrium distance of  $\sigma = 0.3083 \text{ nm}$ . Following [16], the potential well-depth for the interaction between graphene layer and flake is  $\epsilon = 2.968 \text{ meV}$ , and the equilibrium distance is  $\sigma = 0.3407 \text{ nm}$ .

At the beginning, the graphene layer was positioned on top of the undulated copper substrate. A static energy relaxation was first performed in order to minimize the energy of the system. Next, the atomic model was dynamically equilibrated for 200 ps within the framework of a canonical ensemble (NVT), and a Nosé-Hoover thermostat [26,27] was used to control the temperature at 300.0 K. After the equilibration, the graphene layers conformed well with the substrate, such that the

undulation of the copper substrate was transferred to the graphene layer. Then, the graphene flake was positioned at one of the ends of the substrate. In order to start with the flake at a fixed position, the  $y$ -coordinate of the atoms at one edge of the flake was constrained. The whole system was further equilibrated at 300 K for another 50 ps. After the thermodynamic equilibration, the graphene flake also conformed well with the substrate and became undulated, as shown in Fig. 1b. Following equilibration, the microcanonical ensemble (NVE) was employed for the whole atomic system, and the temperature was adjusted by a thermostat of the Berendsen type [28] with damping parameter  $\tau = 0.2 \text{ ps}$ . Simulations were also performed (but not shown here) without the use of a thermostat, and results demonstrated that the presence of the thermostat affects the oscillation of the flake only negligibly. The simulation started when the constraint at the boundary of the flake was removed, and the motion of the flake initiated toward the direction of decaying amplitude, i.e., toward the center of the substrate.

### 3. The oscillatory motion of the flake

Several representative positions of the graphene flake at different simulation times are shown in Fig. 2. At the beginning of the simulation, the graphene flake is positioned at one end of the substrate. Its motion is initially restricted by blocking the displacement of one of its edges. Both the graphene flake and the graphene layer well conform to the undulated profile of the substrate. Therefore, the flake has a periodic out-of-plane bending deformation of magnitude that decreases when going from the border of the substrate toward its center (Fig. 2a). When the edge of the flake is released, the flake starts to move toward the direction with decaying amplitude (Fig. 2b). As the flake moves to the middle region of the substrate where the amplitude is lowest, its translational velocity reaches a maximum (Fig. 2c). After crossing the middle region, the flake continues to move forward toward a region of increasing amplitude, albeit with decreasing velocity (Fig. 2d). When the velocity vanishes, the flake reaches the other end of the substrate (Fig. 2e). At this point the gradient in amplitude induces the flake to revert its motion (Fig. 2d), and the whole process repeats until the dissipation due to friction fully damps the motion of the flake. Indeed, owing to friction, the position reached at the end of each period is not the same as the initial position but progressively closer to the center of the substrate.

Fig. 3 records the position (a), the velocity (b), and the acceleration (c) of the mass center of the flake during the simulation. It is clear that the flake oscillates around the middle of the substrate, with oscillation amplitude gradually decreasing with time and that the velocity is maximum when the acceleration is minimum and vice versa. When the flake

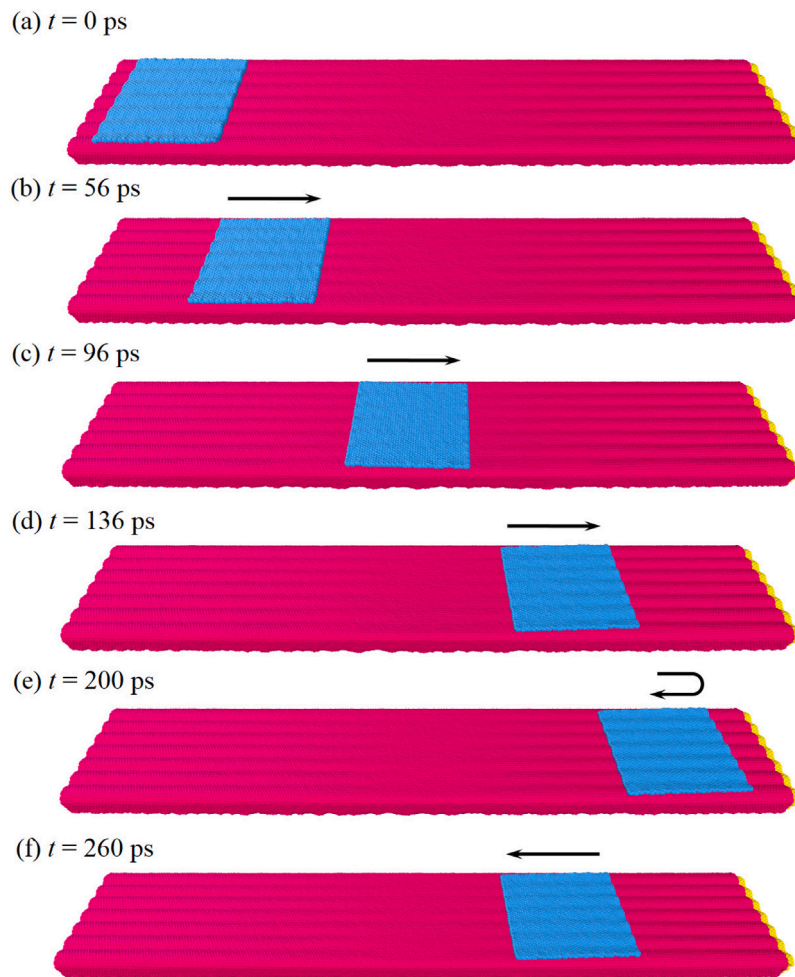


Fig. 2. At different simulation times as shown in (a) ~ (f), the graphene flake moves to different positions.

moves horizontally, its rotation angle with respect to the  $z$ -direction varies in a small range, between  $-3.0$  and  $3.0$  degree, indicating that the flake does not change into a commensurate state with the substrate, so that the static friction between the flake and the substrate remains constant and low at all times.

The periodic oscillation of the flake is a result of the conversion between the potential energy and kinetic energy of the atomic system. The total potential energy  $U_{\text{tot}}$  of the atomic structure can be expressed as follows

$$U_{\text{tot}} = U_{\text{bond}} + U_{\text{bend}} + U_{\text{interfacial}} \quad (3)$$

where  $U_{\text{bond}}$  refers to the atomic bonding energies of the individual components, copper substrate, graphene layer and graphene flake,  $U_{\text{bend}}$  refers to the bending elastic energy of the graphene layer and that of the flake, and  $U_{\text{interfacial}}$  to the interfacial potential energy between flake and coated substrate, which comprises the interaction between flake and graphene layer, graphene layer and copper substrate, and also copper substrate and graphene flake. When the flake moves, there is no occurrence of bond-breaking or rebonding, so that the first term is constant. The only terms in Eq. (3) that change significantly while the slider moves are the elastic bending energy of the graphene flake and the interfacial energy between the flake and the coated layer. Variations in bending energy and elastic energy translate into a variation of the kinetic energy, and partially into heat because of friction (see in Fig. 4 how the quantities oscillate during the simulation). When the sum of the interfacial and elastic bending energy decreases, the kinetic energy of the flake increases, indicating that the potential energy is

transformed into kinetic energy, and vice versa. The attractive energy between flake and layer decreases when the flake moves from the end of the substrate to the middle, because the substrate becomes flatter and the two surfaces get closer. While both the kinetic energy and the interfacial energy exhibit a regular oscillation, the bending energy has a less regular pattern (see Fig. 4). This is due to the random in-plane rotation of the flake, which induces an irregular release of the elastic energy.

The interfacial force distribution of the flake is shown in Fig. 6(b) for three representative positions indicated in Fig. 6(a): the two ends of the substrate and its middle. The substrate has a higher local undulation in the region close to the two ends, and a lower local undulation in the middle region. Thus, the flake becomes relatively flat when it moves to the middle region.

The interfacial force is calculated at a specific time, by first freezing the instantaneous morphology of the atomic structure. Then, the calculation of the interfacial force acting on an atom of the flake is performed by adding the contributions of the atoms that are in the graphene layer, covering the substrate, and the copper atoms that are inside of the cut-off radius.

Note that the atomic forces mainly concentrate around the higher parts of the undulations where the curvature is largest. When the flake is in the middle region, the negative and positive forces are nearly homogeneously distributed among the flake atoms, which result in a zero net force. The force distribution originates from the fact that the amplitude gradient mainly varies along the ‘ridges’ of the flake.

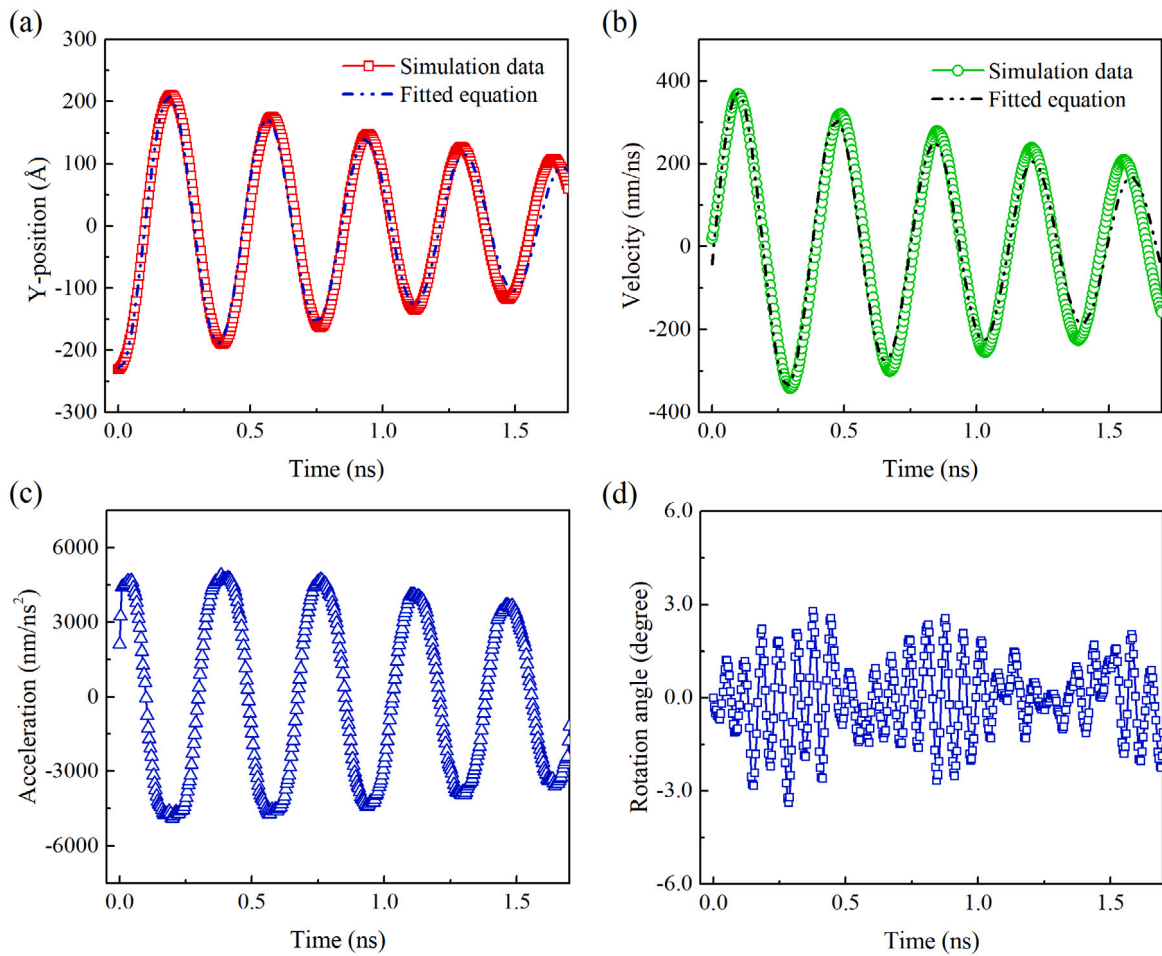


**Fig. 3.** (a) The position of the flake mass center changes with time. In (b), (c) and (d), the variation of the velocity, acceleration and rotation angle of the flake with respect to time are depicted. In the figures, the dash-dot-dot lines are the results of theoretical model.

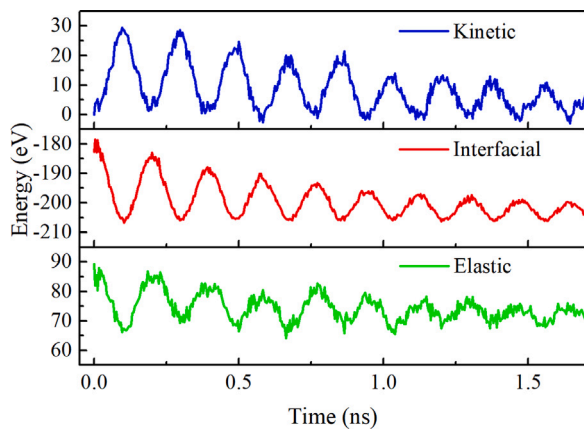


**Fig. 4.** The variation of the kinetic energy, the interfacial energy, and the elastic bending energy of the flake with respect to simulation time.

#### 4. The equation of motion of the flake

The equation of motion of the flake can be approximated as

$$m\ddot{y} = F_p + F_f, \quad (4)$$

where  $m$  is the flake mass,  $y$  is the position of its center of mass,  $F_p$  is the driving force and  $F_f$  is the friction force. The friction force is known

to be proportional to the velocity as  $F_f = -\gamma \dot{y}$ , with  $\gamma$  the damping coefficient.

In the assumption that the flake can be regarded as a body with a single degree of freedom, the driving force with respect to the  $y$ -coordinate can be derived from Eq. (3) as

$$F_p = -\frac{dU_{\text{tot}}}{dy} = -\frac{dU_{\text{bi}}}{dy} = -\frac{d(U_{\text{bend}} + U_{\text{interfacial}})}{dy}. \quad (5)$$

Here,  $U_{\text{bi}}$  represents the sum of the bending and interfacial energies.

In Fig. 5a and b the variations of the bending energy and of the interfacial energy are shown as a function of position, when the flake moves from one end of the substrate to the other. For both energies the data points can be well fitted by a quadratic function. Previous studies demonstrated that the bending energy of graphene can be approximated by a function of curvature  $\kappa$ ,  $U_{\text{bend}} = \alpha\kappa^2$ , where  $\alpha$  is a material-dependent constant [29]. In these simulations the curvature of the flake is not constant, but decreases with the amplitude of the substrate, and, on average, decreases with  $y$ . The interfacial Van der Waals potential energy is also linked to curvature, as demonstrated also by [15] and from Fig. 5a does also depend quadratically on  $y$ . Therefore, the data for the bending and interfacial energy  $U_{\text{bi}}$  can be described by a parabolic function of the form

$$U_{\text{bi}}(y) = ay^2 + b \quad y_l \leq y \leq y_h, \quad (6)$$

where  $a$  and  $b$  are fitting parameters,  $y_l$  and  $y_h$  are the lower and upper bounds of the slip path of the flake. By substituting Eq. (6) into Eq. (5), the driving force is found to be  $F_p = -dU_{\text{tot}}/dy = ky$ . The value of  $k$  can be obtained by fitting the interfacial force distribution in Fig. 5d,

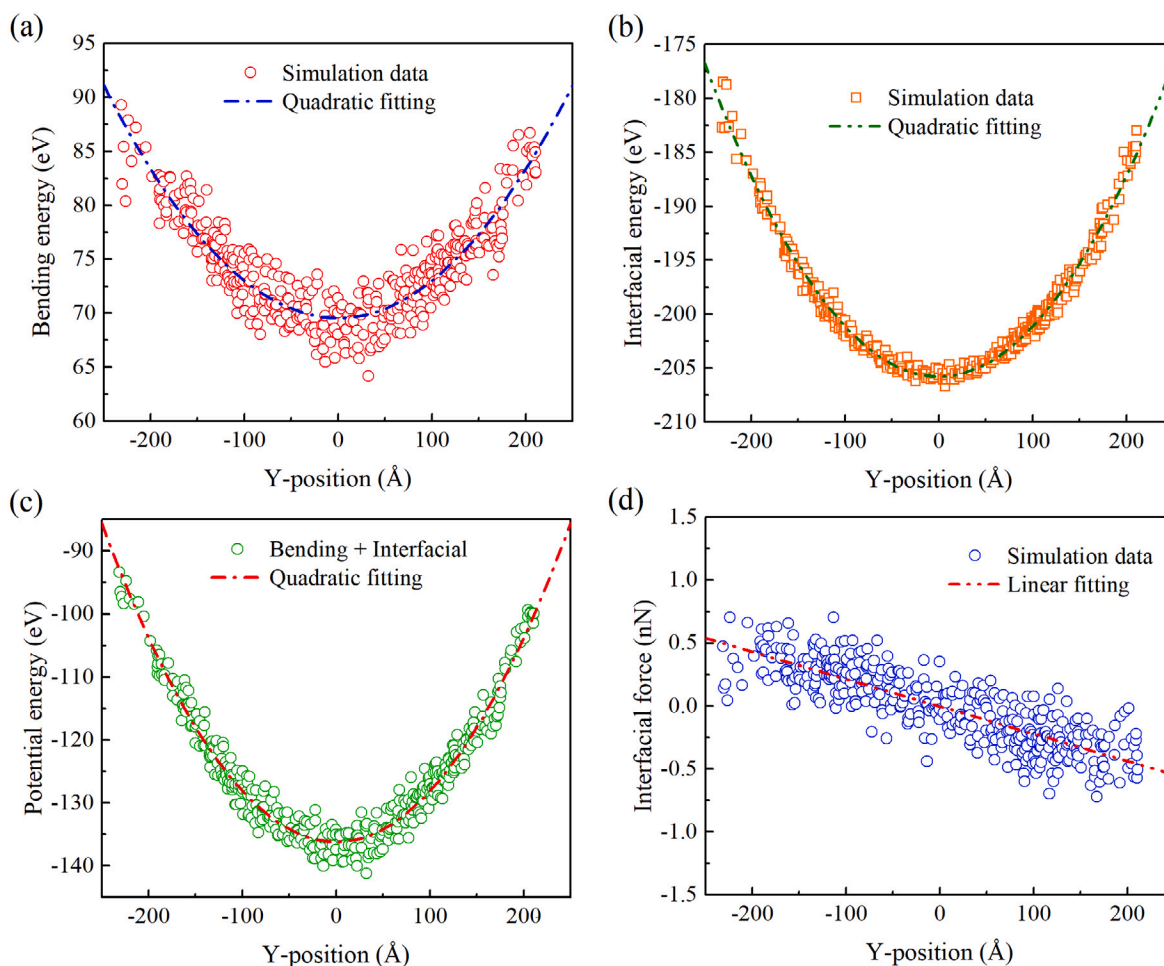


Fig. 5. The variation of the (a) bending energy, (b) the interfacial energy, (c) the potential energy, and (d) the interfacial force versus the position of the mass center of the flake. The dash-dot-dot lines are the quadratic and linear fittings of the data points.

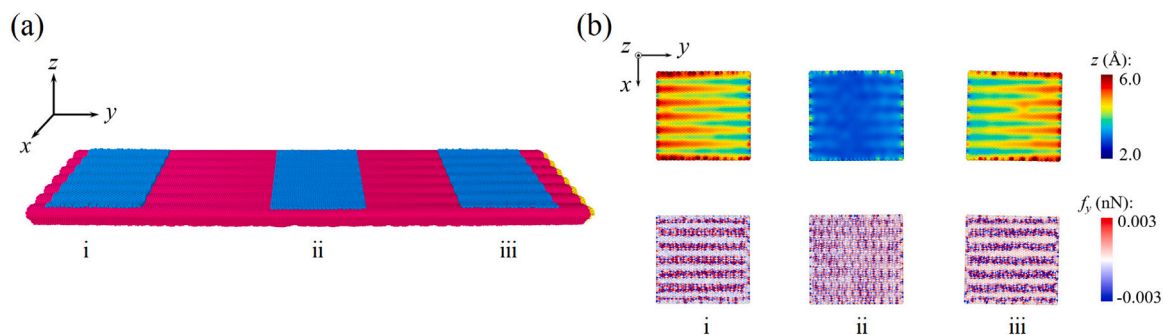


Fig. 6. (a) Positions of the flake on the substrate where (b) the height of the flake and the interfacial force distribution are calculated.

which can be well approximated by a linear function passing through zero when the flake is in the middle of the substrate. The fitted value of  $k$  is  $0.0217 \text{ N/m}$ . The scatter in the data points is caused by the fact that the flake does not have more than a single degree of freedom, and does both rotate around the  $z$ -direction and vibrate along the  $x$ -direction.

The damping coefficient  $\gamma$  can instead be obtained by fitting the decaying oscillation magnitude in Fig. 3a, and is found to be  $0.0804 \text{ pN s/m}$ . Fig. 3a and b compare the flake trajectory predicted by Eq. (4)

with the fitted coefficients and the simulation data. The agreement confirms that the movement of the flake on a substrate with an undulation with amplitude gradient can be well described by a damped harmonic oscillator.

The frequency of the flake oscillation can be tuned by changing the gradient of the amplitude. Fig. 7a shows how the amplitude gradient, ranging between  $1.5$  and  $9.0 \times 10^{-3}$ , influences the oscillation frequency. Note that a larger amplitude gradient leads to a higher oscillation frequency of the graphene flake. A linear relationship between

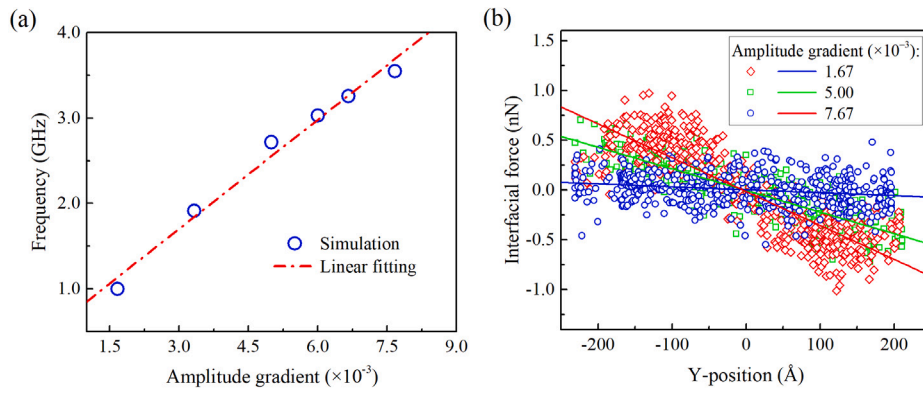


Fig. 7. (a) The oscillation frequency of the flake with the amplitude gradient. A dashed-dotted line indicates the linear behavior of an harmonic oscillator. (b) The variation of the interfacial force with the amplitude gradient. Open symbols are the simulation data, the lines are the linear fits.

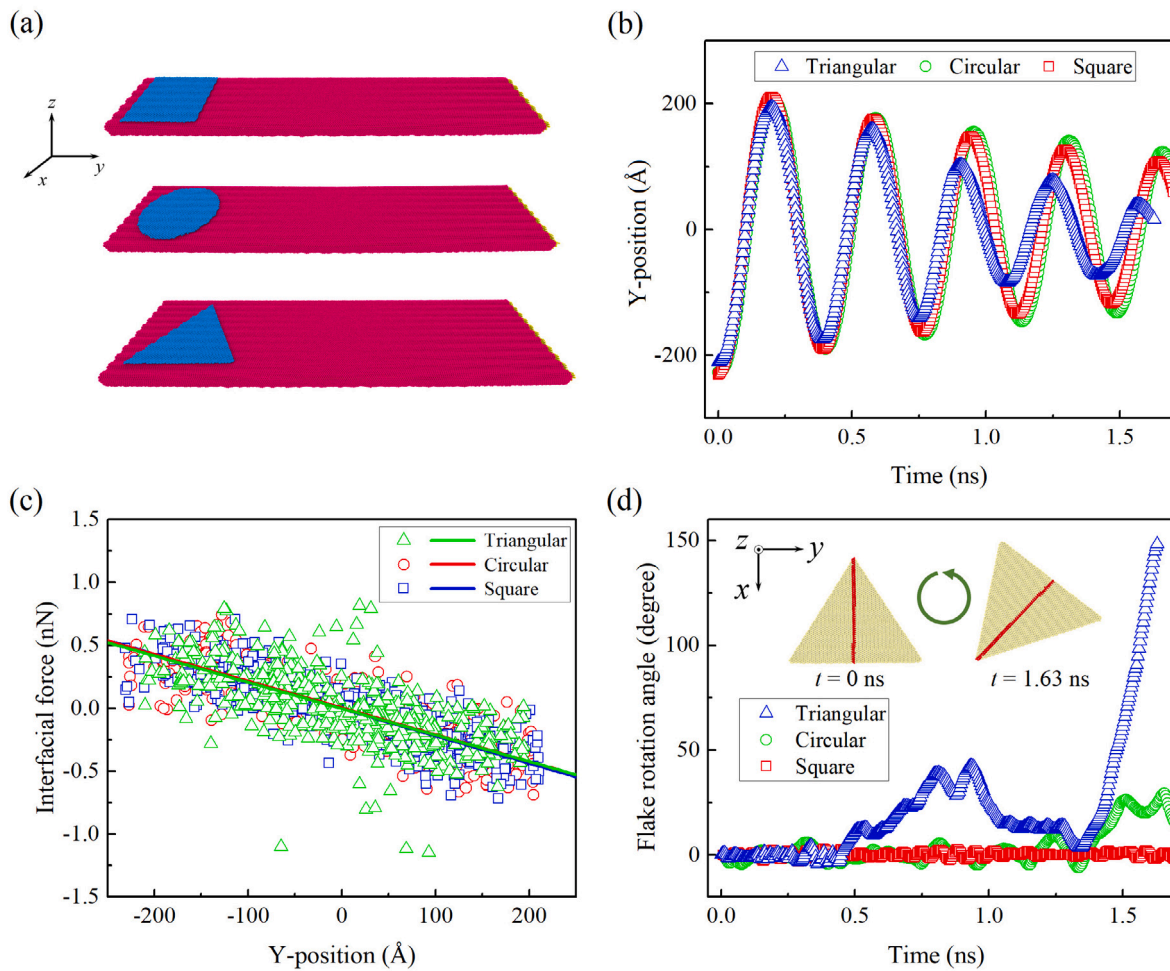


Fig. 8. (a) Three models with flakes of different shape. (b) The variation of the flake position versus time. (c) The dependence of the interfacial force on flake position. In the figure, open symbols are simulation data, solid lines are fits. (d) The variation of flake rotation angle versus time.

frequency and amplitude gradient is to be expected when friction is negligible (the damping coefficient is very small) and the behavior of the flake can be approximated to that of an harmonic oscillator, with its typical frequency  $\omega = \sqrt{\frac{k}{m}}$ . This can be seen by noting that the energy of the flake depends on the square of the curvature  $\kappa$  [29] as

$$U = \alpha \iint \kappa^2(x, y) dx dy; \quad (7)$$

where  $\alpha$  is a material constant, and that the curvature for small  $g$  can be approximated as being linear in  $g$ :

$$\kappa(x, y) = gy \frac{\omega^2 \cos(\omega x)}{[1 + g^2 \omega^2 \sin^2(\omega x)]^{\frac{3}{2}}} \approx gy f(x). \quad (8)$$

Therefore, the driving force is

$$F = -ky = -\frac{\partial U}{\partial y} = -Cg^2 y. \quad (9)$$

where  $C$  is a constant that depends on the material and dimensions of the flake.

Clearly, in our simulations friction is non-negligible, or motion would not be damped. This constitutes a deviation from linearity: when the amplitude gradient is larger, the driving force and the velocity are also larger, so is friction. Also, with increasing amplitude gradient, the curvature increases and does no longer depend on gradient quadratically, thus there is an additional deviation from linearity.

Fig. 7b shows that the interfacial force experienced by the flake varies almost linearly with the position of the flake. The slope of the fitted line increases with amplitude gradient.

## 5. Shape of the flake

To explore the influence of the flake shape on the oscillation, the simulations in the previous section are repeated for three different flake shapes, square, circular and triangular, as shown in Fig. 8a. The areas of all the flakes are the same, to ensure that the friction coefficient is comparable. Fig. 8b depicts the variation of the flake position with respect to time. It is shown that, when the flake has a circular or square shape, the curves approximately overlap. However, when the flake is triangular, the magnitude of the oscillation decays much faster than in the other two cases, indicating larger dissipation. As shown in Fig. 8c, the dependence of the interfacial force on the flake position exhibit similar trends for all the three different flake shapes. However, the force distribution is scattered in a larger range when the flake has a triangular shape. Indeed, Fig. 8d shows that the triangular flake has the largest rotation angle compared to the other two cases. Because of the rotation, more energy is dissipated through friction and, as a result, the oscillation magnitude in  $y$ -direction decays faster.

## 6. Conclusions

In the present study, the oscillation of a graphene flake on an undulated substrate with varying amplitude, covered with a conforming graphene sheet, is explored using MD simulation. The motion of the flake closely resembles that of a damped harmonic oscillator. The potential energy that transforms in kinetic energy is provided by the elastic bending energy of the flake which decrease with decreasing curvature and by the Van der Waals interaction between flake and graphene which also decreases with curvature. Interfacial friction is the damping term which dissipates energy, and decreases the amplitude of oscillation. Since the rotational energy is negligible for flakes with square or circular shape, the alignment between flake and sheet is never commensurate, and the friction coefficient very small. Only for triangular flakes, the rotational frequency is non-negligible and adds to the losses due to friction. The oscillation frequency is found to linearly increase with the amplitude gradient. The present study supplies an alternative approach to guide the motion of nanoscale objects on substrates, and has the potentials to be exploited in the design of nanoelectro-mechanical systems.

### CRedit authorship contribution statement

**Jianjun Bian:** Conceptualization, Software, Data analysis, Data curation, Investigation, Writing – original draft. **Lucia Nicola:** Conceptualization, Supervision, Writing – review & editing, Funding acquisition.

### Data availability

This study is based only on data obtained using the methods described in this paper, it is therefore readily reproducible.

## Acknowledgments

This project has received funding from the European Research Council (ERC) under the European Union's Horizon 2020 research and innovation programme (grant agreement no. 681813). Professor G.F. Wang of the Xi'an Jiaotong University is gratefully acknowledged for having granted J.B. the use of the computer facilities of his group.

## References

- [1] O. Akhavan, M. Saadati, M. Jannesari, Graphene jet nanomotors in remote controllable self-propulsion swimmers in pure water, *Nano Lett.* 16 (2016) 5619–5630.
- [2] M. Jannesari, O. Akhavan, H.R.M. Hosseini, B. Bakhsi, Graphene/CuO<sub>2</sub> nanoshuttles with controllable release of oxygen nanobubbles promoting interruption of bacterial respiration, *ACS Appl. Mater. Interfaces* 12 (2020) 35813–35825.
- [3] X. Ma, J. Katuri, Y. Zeng, Y. Zhao, S. Sanchez, Surface conductive graphene-wrapped micromotors exhibiting enhanced motion, *Small* 11 (38) (2015) 5023–5027.
- [4] Wang, H., M. Pumera, Fabrication of micro/nanoscale devices, *Chem. Rev.* 115 (2015) 8704–8735.
- [5] O. Akhavan, E. Ghaderi, The use of graphene in the self-organized differentiation of human neural stem cells into neurons under pulsed laser stimulation, *J. Mater. Chem. B* 2 (2014) 5602–5611.
- [6] J.W. Kang, H.J. Hwang, Nanoscale carbon nanotube motor schematics and simulations for micro-electro-mechanical machines, *Nanotechnology* 15 (2004) 1633–1638.
- [7] A.M. Fennimore, T.D. Yuzvinsky, W. Han, M.S. Fuhrer, J. Cumings, A. Zettl, Rotational actuators based on carbon nanotubes, *Nature* 424 (2003) 408–410.
- [8] K.F. Rinne, S. Gekle, D.J. Bonthuis, R.R. Netz, Nanoscale pumping of water by AC electric fields, *Nano Lett.* 12 (2012) 1780–1783.
- [9] A. Nourhani, V.H. Crespi, P.E. Lammert, Guiding chiral self-propellers in a periodic potential, *Phys. Rev. Lett.* 115 (2015) 118101.
- [10] S.C. Hernandez, C.J.C. Bennett, C.E. Junkermeier, S.D. Tsoi, F.J. Bezares, S. Stine, J.T. Robinson, E.H. Lock, D.R. Boris, B.D. Pate, J.D. Caldwell, T.L. Reinecke, P.E. Sheehan, S.G. Walton, Chemical gradients on graphene to drive droplet motion, *ACS Nano* 7 (2013) 4746–4755.
- [11] M. Becton, X. Wang, Thermal gradients on graphene to drive nanoflake motion, *J. Chem. Theory Comput.* 10 (2014) 722–730.
- [12] P.M. Shenai, Z. Xu, Y. Zhao, Thermal-gradient-induced interaction energy ramp and actuation of relative axial motion in short-sleeved double-walled carbon nanotubes, *Nanotechnology* 22 (2011) 485702.
- [13] J. Leng, Y. Hu, T. Chang, Nanoscale directional motion by angustotaxis, *Nanoscale* 12 (2020) 5303.
- [14] Y. Huang, S. Zhu, T. Li, Directional transport of molecular mass on graphene by straining, *Extreme Mech. Lett.* 1 (2014) 83–89.
- [15] C. Dai, Z. Guo, H. Zhang, T. Chang, A nanoscale linear-to-linear motion converter of graphene, *Nanoscale* 8 (2016) 14406–14410.
- [16] T. Chang, H. Zhang, Z. Guo, X. Guo, H. Gao, Nanoscale directional motion towards regions of stiffness, *Phys. Rev. Lett.* 114 (2015) 015504.
- [17] L.D. Machado, R.A. Bizao, N.M. Pugno, D.S. Galvao, Controlling movement at nanoscale: curvature driven mechanotaxis, *Small* 2100909 (2021) 1–9.
- [18] Q. Flamant, A.M. Stancius, H. Pavailler, C.M. Sprecher, M. Alini, M. Peroglio, M. Anglada, Roughness gradient on zirconia for rapid screening of cell-surface interface: fabrication, characterization and application, *J. Biomed. Mater. Res. A* 104 (2016) 2502.
- [19] Y. Hou, W. Xie, L. Yu, L.C. Camacho, C. Nie, M. Zhang, R. Haag, Q. Wei, Surface roughness gradient reveal topography-specific mechanosensitive responses in human mesenchymal stem cells, *Small* 1905422 (2020) 1–10.
- [20] C. Lv, P. Hao, Driving droplet by scale effect on microstructured hydrophobic surfaces, *Langmuir* 28 (2012) 16958–16965.
- [21] S. Bidmeshkipour, O. Akhavan, P. Salami, L. Yousefi, A periodic perforated graphene in optica nanocavity absorbers, *Mater. Sci. Eng. B* 276 (2022) 115557.
- [22] B. Luan, M.O. Robbins, The breakdown of continuum models for mechanical contacts, *Nature* 435 (2005) 929–932.
- [23] Z. Ye, A. Balkanci, A. Martini, M.Z. Baykara, Effect of roughness on the layer-dependent friction of few-layer graphene, *Phys. Rev. B* 96 (2017) 115401.
- [24] S.J. Stuart, A.B. Tutein, J.A. Harrison, A reactive potential for hydrocarbons with intermolecular interactions, *J. Chem. Phys.* 112 (2000) 6472.
- [25] J. Bian, L. Nicola, On the lubrication of rough copper surfaces with graphene, *Tribol. Int.* 156 (2021) 106837.
- [26] S.A. Nosé, A unified formulation of the constant temperature molecular dynamics methods, *J. Chem. Phys.* 81 (1984) 511–519.
- [27] W.G. Hoover, Canonical dynamics: Equilibrium phase-space distributions, *Phys. Rev. A* 31 (1985) 1695–1697.
- [28] H.J.C. Berendsen, J.P.M. Postma, W.F. van Gunsteren, A. DiNola, J.R. Haak, Molecular dynamics with coupling to an external bath, *J. Chem. Phys.* 81 (1984) 3684.
- [29] T. Ma, B. Li, T. Chang, Chirality-and curvature-dependent bending stiffness of single layer graphene, *Appl. Phys. Lett.* 99 (2011) 201901.